

Stimulus-dependent correlations and population codes

Krešimir Josić
 Department of Mathematics
 University of Houston
 Houston TX 77204-3008, USA

Eric Shea-Brown
 Department of Applied Mathematics
 University of Washington
 Seattle, WA 98195-2420

Brent Doiron
 Department of Mathematics
 University of Pittsburgh
 Pittsburgh, PA, 15206

Jaime de la Rocha
 Center for Neural Science
 New York University
 New York NY 10012, USA

June 2, 2018

Abstract

The magnitude of correlations between stimulus-driven responses of pairs of neurons can itself be stimulus-dependent. We examine how this dependence impacts the information carried by neural populations about the stimuli that drive them. Stimulus-dependent changes in correlations can both carry information directly and modulate the information separately carried by the firing rates and variances. We use Fisher information to quantify these effects and show that, although stimulus dependent correlations often carry little information directly, their modulatory effects on the overall information can be large. In particular, if the stimulus-dependence is such that correlations increase with stimulus-induced firing rates, this can significantly enhance the information of the population when the structure of correlations is determined solely by the stimulus. However, in the presence of additional strong spatial decay of correlations, such stimulus-dependence may have a negative impact. Opposite relationships hold when correlations decrease with firing rates.

1 Introduction

The impact of correlations on information encoded in neural tissue is a subject with a substantial history. We start our discussion with [49], which reported significant correlations between neuronal responses in paired recordings of neurons in the visual area of monkeys. Correlations were deemed undesirable, as they lead to a *decrease* in the signal-to-noise ratio of the summed population activity [24, 9]. Despite this impact on the signal-to-noise ratio, correlations in the neural response can *increase* the information that a population of neurons carries about a signal [1]. The impact of correlations on coding depends in a complex way on their distribution over the neuronal population [37, 13, 34, 31, 3, 40, 27, 1, 43, 44, 46]. As the range of potential patterns of correlation is vast, and has not been characterized in most neurobiological systems, the effect of correlations is not fully understood.

In many studies to date, the correlation coefficient between the responses of pairs of neurons was assumed to be independent of the stimulus driving the response. In particular, it was assumed

that covariances between cell responses change together with the variance so that the correlation coefficient remained constant. Information about stimulus identity could then be encoded solely in the rate and variability of single cell responses [1, 43, 44, 46]. However, experimental findings suggest that correlations themselves vary with stimuli [18, 38, 26, 17, 21, 17, 7, 11]. More specifically, it has been shown in [26] that correlations in the visual cortex (V1) vary with the stimulus orientation and contrast. In [7], it was demonstrated experimentally that in certain situations changes in perceived brightness are related to changes in neural correlations. Responses to prey-like vs. conspecific-like stimuli in electric fish have also been demonstrated to evoke responses with different correlation structure [11].

Here, we concentrate on a particular form of stimulus-dependence, in which correlations depend on stimulus-evoked firing rates (although many of our formulas hold more generally). In recent work, we have shown that spike-to-spike correlations due to common inputs increase with firing rate for neural models and *in vitro* neurons [17]. This effect was observed *in vivo* in the anesthetized visual cortex [26, 22] and, in certain experimental regimes, for motoneurons *in vitro* [8]. In the oculomotor neural integrator the opposite effect was observed: correlations decreased with rate [2], perhaps due to recurrent network interactions. We will study both of these cases, illustrating strongly differing effects of stimulus-dependence in each.

The goal of this paper is to examine, from a theoretical perspective, the impact of stimulus-dependent correlations on population coding. Previously, changes in discriminability due to changes in the covariance matrix of pairs of cells and small (3-8 cell) ensembles were examined by [6]. Also, a series expansion of mutual information to isolate and quantify the effects of stimulus-dependent correlations has been developed [32]. Similarly, [30] use mutual information to assess the impact of tuned correlations measured in primate V1. We take a somewhat different approach based on computing the impact of the stimulus dependence of correlations on the Fisher information (I_F) for populations of neurons whose response is described by tuning curves [1].

There are at least two distinct ways in which the stimulus dependence of correlations can impact Fisher information. First, the fact that patterns of correlation across a population are adjusted as stimuli change can have a strong “modulatory” impact on the information that *other* features of the neural response – such as firing rates – carry about the stimulus [30, 23]. We refer to this effect as *correlation shaping*. To better understand this, note that a stimulus-independent correlation structure may be optimized for one stimulus. However, stimulus-dependence offers the possibility that the correlation structure is adjusted, and optimized, for a range of stimuli [3]. In a related effect, adaptation has been shown to modify correlation structure and increase I_F [27, 23].

Secondly, information may be encoded directly by changes in the level of correlation between neurons, in addition to encoding via changes in firing rate and variance. We refer to this mechanism as *correlation coding*. One scenario where correlation coding clearly dominates if stimuli *only* affect the correlation structure, leaving rates and variances relatively constant, as has been observed experimentally [47, 7, 11].

The balance of the paper proceeds as follows. We start by defining our statistical description of the neural response to stimuli in Section 2. The information in the response of two cells is studied in Section 3. As we show, the insights gained from this case can be extended to small populations, but do not always apply to larger populations. In Section 4 we study the information in the response of a large population. Here, we find that correlation shaping effects can be substantial, and often dominate over correlation coding. In Section 5 we extend the model to address additional structure of correlations across the population, by including decay of correlations that depends explicitly on

the spatial or “functional” distance between preferred stimuli of neurons, as shown experimentally. We find that the impact of correlation shaping in the presence of such a decay continues to be strong, but that correlation coding also plays a significant role. We conclude with a discussion of the results. A number of analytical results used in the main body of the paper, which may be of independent interest, are derived in the appendices.

2 Setup

Structure of correlations We consider a population of N neurons responding to a stimulus described by a scalar variable θ (for example, the orientation of a visual grating). The number of spikes fired by neuron i in response to stimulus θ during a fixed time interval is given by

$$r_i(\theta) = f_i(\theta) + \eta_i(\theta), \quad (1)$$

where $f_i(\theta)$ is the mean response of neuron i across trials, and $\eta_i(\theta)$ models the trial-to-trial variability of the response. We use boldface notation for vectors, so that $\mathbf{r}(\theta)$ denotes the multivariate random variable $\mathbf{r}(\theta) = [r_1(\theta), r_2(\theta), \dots, r_N(\theta)]^T$. For simplicity, we sometimes suppress dependences on θ .

We assume that $\boldsymbol{\eta}$ follows a multivariate distribution with zero mean and covariance matrix $\mathbf{Q}(\theta)$ defined by

$$Q_{i,j}(\theta) = \delta_{i,j}v_i(\theta) + (1 - \delta_{i,j})\rho_{i,j}(\theta)\sqrt{v_i(\theta)v_j(\theta)}. \quad (2)$$

Here $v_i(\theta)$ is the variance of the response of cell i , and $-1 \leq \rho_{i,j}(\theta) \leq 1$ is the correlation coefficient of the response of cells i and j . Although most of our results will be discussed in the range of small to intermediate correlations, $\rho_{i,j} \lesssim 0.5$, a similar analysis can be used to study the behavior of populations close to perfect correlations, $\rho_{i,j} \approx 1$. Assumptions on the form of the distribution, beyond this covariance, are made only where needed.

For studies of stimulus-dependent correlations in small-to-intermediate populations (Section 3), we will allow for general forms of $\rho_{i,j}(\theta)$. When we study large populations (Sections 4 and 5), we will assume that

$$\rho_{i,j}(\theta) = S_{i,j}(\theta) c(\phi_i - \phi_j), \quad (3)$$

where ϕ_i and ϕ_j are the preferred stimuli of neurons i and j respectively. The stimulus independent term $c(\phi_i - \phi_j)$ represents the *spatial or functional* structure of correlations in the population. It describes how correlations vary across the population according to their preferred stimuli, perhaps due to hardwired differences in the level of shared inputs. For instance, neurons which prefer similar stimuli are frequently closeby in the cortex, and may share a larger number of common inputs than neurons that exhibit different preferences [49, 28]. Moreover, the set of neurons upstream of two cells with similar stimulus preferences may also undergo common fluctuations in their activity. Therefore, $c(\phi_i - \phi_j) = c(\Delta\phi)$ is frequently assumed to decrease with the functional distance $\Delta\phi$. We will refer to this simply as “spatial decay” [16, 46, 48].

We emphasize that it is the stimulus dependence of the correlation coefficient, $\rho_{i,j}(\theta)$, that distinguishes the present work from several previous investigations [1, 46, 43]. This dependence enters through the term $S_{i,j}(\theta)$ [26, 17, 22]. We mainly investigate cases in which correlations between pairs of cells increase, decrease, or have a single maximum with respect to the evoked firing rates f_i and f_j [17, 45, 26, 8, 2]. However, our results could also be applied to cases with

other relations between $\rho_{ij}(\theta)$, f_i , f_j , v_i , and v_j such as those arising for different circuit and nonlinear spike generation mechanisms (cf. Fig. 4 of [17]).

For large populations, we extend the multiplicative model in [42] to the case of stimulus-dependent correlations by assuming that

$$S_{i,j}(\theta) = s_i(\theta)s_j(\theta), \quad (4)$$

where $-1 < s_i(\theta), s_j(\theta) < 1$. Here $s_i(\theta)$ may be thought of as the propensity of a neuron's response to be correlated, and $s_i^2(\theta)$ as the correlation between two neurons which respond equivalently to the stimulus. There are several reasons for adopting the form given in Eq. (4). Firstly, this form of ρ_{ij} arises for small to intermediate correlation in neuron models producing a spike train with renewal statistics [17, 45]. Moreover, in this case correlation has also been shown to vary with the geometric mean of the firing rate of pairs of cells *in vivo* [26, 17], which can be modeled using Eq. (4). Additionally, this form keeps the computations at hand analytically tractable for large population sizes, and limits the number of cases under study.

Fisher information To quantify the fidelity with which a neuronal population represents a signal, we use Fisher information [41, 16]. For the probability distribution $p[\mathbf{r}|\theta]$ of the spike count vector \mathbf{r} given stimulus θ , the Fisher information is defined as

$$I_F(\theta) = \left\langle -\frac{d^2}{d\theta^2} \log p[\mathbf{r}|\theta] \right\rangle,$$

where $\langle \cdot \rangle$ denotes expectation over the responses \mathbf{r} . The inverse of the Fisher information, $1/I_F(\theta)$, provides a lower bound on the variance (i.e., an upper bound on the accuracy) of an unbiased decoding estimate of θ from the population response [14, 16]. Fisher information is directly related to the discriminability d' between two stimuli θ and $\theta + \Delta\theta$, since $d' \approx \Delta\theta \sqrt{I_F(\theta)}$ for small $\Delta\theta$ [16].

The Fisher information can be written as [25]

$$I_F = I_F^{\text{mean}} + I_F^{\text{cov}}. \quad (5)$$

Here

$$I_F^{\text{mean}} = \mathbf{f}'^T \mathbf{Q}^{-1} \mathbf{f}' \quad (6)$$

is known as the “linear approximation” to the Fisher information, or the linear Fisher information. Specifically, the inverse of $\mathbf{f}'^T \mathbf{Q}^{-1} \mathbf{f}'$ gives the asymptotic¹ error of the optimal linear estimator of the stimulus, for a response to the stimulus that follows *any* response distribution that has mean $\mathbf{f}(\theta)$ and covariance $\mathbf{Q}(\theta)$ [35, 15, 40]. In particular, this applies to gaussian or nongaussian distributions.

The second term, I_F^{cov} , does depend on the the form of the response distribution, beyond its covariance. In the following, whenever computing I_F^{cov} , we assume that $\boldsymbol{\eta}$ follows a multivariate

¹Here, asymptotic implies that the optimal linear estimator is constructed based on full knowledge of the mean and covariance of the underlying stimulus-response distributions.

Gaussian distribution, so that [25]

$$I_F^{\text{cov}} = \frac{1}{2} \text{Tr} [\mathbf{Q}' \mathbf{Q}^{-1} \mathbf{Q}' \mathbf{Q}^{-1}]. \quad (7)$$

As we explain below, correlation coding affects only I_F^{cov} , while correlation shaping affects both I_F^{mean} and I_F^{cov} .

3 The cases of cell pairs and small populations

We start by considering the impact of correlations on the information carried by cell pairs, and small populations ($N < 1/\rho$). This was the setting of many experimental studies which addressed the role of correlations in the neural code [33, 4, 36, 39, 34, 23]. We use analytical expressions to show that, depending on correlation structure, correlation shaping can have either a positive or negative impact on I_F^{mean} . Most beneficial are high correlations between neurons with different stimulus preferences, and low correlations between neurons with similar preferences. For small to intermediate correlations, $I_F^{\text{mean}} \approx I_F$, and hence correlation coding has little effect. These results are in agreement with previous observations [36, 5, 3]. We emphasize that these results can be expected to hold only when $N < 1/\rho$: in subsequent sections we show that the intuition gained from studying cell pairs may not always extend to larger populations.

Fisher information in cell pairs We first consider two cells whose response follows a bivariate Gaussian distribution given by Eqs. (1–2). For two neurons, we write the correlation coefficient as $\rho_{1,2} = \rho_{2,1} = \rho$, and obtain

$$I_F = \underbrace{\frac{1}{1-\rho^2} \left[\frac{f'_1}{\sqrt{v_1}} - \frac{f'_2}{\sqrt{v_2}} \right]^2 + \frac{2}{1+\rho} \left[\frac{f'_1 f'_2}{\sqrt{v_1 v_2}} \right]}_{I_F^{\text{mean}}} + \underbrace{\frac{2-\rho^2}{4(1-\rho^2)} \left[\left(\frac{v'_1}{v_1} \right)^2 + \left(\frac{v'_2}{v_2} \right)^2 \right] - \frac{\rho^2}{2(1-\rho^2)} \frac{v'_1 v'_2}{v_1 v_2} + \left[\frac{(1+\rho^2)\rho'}{1-\rho^2} \right] \left[\frac{\rho'}{1-\rho^2} - \frac{\rho}{1+\rho^2} \left(\frac{v'_1}{v_1} + \frac{v'_2}{v_2} \right) \right]}_{I_F^{\text{cov}}}, \quad (8)$$

where all derivatives are taken with respect to the stimulus θ .

Intuitively, I_F^{mean} and I_F^{cov} represent the contribution of changes in the firing rate and covariance, respectively, to the Fisher information. While I_F^{mean} has been studied previously, I_F^{cov} has only been examined for stimulus independent correlation coefficients, *i.e.* when $\rho' = 0$ [1, 46, 43, 42]. We separate the influence of stimulus dependent changes in correlation on I_F as follows:

- *Correlation Coding.* The last of the five terms in the sum (8) is only present when $\rho' \neq 0$, and captures the amount of information directly due to changes in correlations [47, 11]. We refer to terms in I_F that are nonzero only when $\rho' \neq 0$ as the contribution of *correlation coding*. If $f'_1 = f'_2 = v'_1 = v'_2 = 0$ then all information is due to correlation coding. It is necessary to use a nonlinear readout (decoding) scheme to recover this information [43].

- *Correlation Shaping.* I_F^{mean} is affected significantly by the level of correlation, ρ . As $(I_F^{\text{mean}})^{-1}$ measures the error in the optimal linear estimate of the stimulus, the impact of changes in correlation structure on I_F^{mean} represents the amount by which correlations *shape* the information available from linear readouts of the response. We refer to this effect as *correlation shaping*.

This terminology anticipates the discussion of larger populations, where we will be interested in how the *spatial structure* together with *stimulus dependent changes* of ρ_{ij} affect I_F . We note that stimulus-dependent correlations can also impact the information available from the variance of the neural response (see the third term in Eq. (8)). This is another form of correlation shaping with a marginal impact in the cases we discuss.

We first examine the effect of correlation shaping. A number of previous studies concluded that an increase in correlation, ρ , can positively impact I_F^{mean} for pairs of neurons that have different “normalized” mean responses to the stimulus ($f'_1/\sqrt{v_1} \neq f'_2/\sqrt{v_2}$). The effect tends to be negative if the responses are similar ($f'_1/\sqrt{v_1} \approx f'_2/\sqrt{v_2}$). Intuitively, correlations can be used to remove uncertainty from noisy responses of neuron pairs with differing response characteristics [31, 3, 1, 46].

Indeed, the first term in Eq. (8), $[f'_1/\sqrt{v_1} - f'_2/\sqrt{v_2}]^2/(1-\rho^2)$, increases with ρ , unless $f'_1/\sqrt{v_1} = f'_2/\sqrt{v_2}$. The resulting increase in discriminability is illustrated in Fig. 1 where we show the bivariate distribution $p(r_1, r_2)$ of the response to two nearby stimuli θ_A and θ_B . In panels a) and b), $v'_1 = v'_2 = \rho' = f'_2 = 0$, but $f'_1 \neq 0$, so that only the first term in I_F^{mean} contributes to I_F . In this example, an increase in correlation leads to a large increase in I_F . In Fig. 1 this increase results in improved discriminability between the stimuli, *i.e.* a reduction of the probability that the two stimuli will lead to the same response. However, when the two neurons respond similarly to the stimulus, $f'_1/\sqrt{v_1} \approx f'_2/\sqrt{v_2}$, the second term, $2[f'_1 f'_2/\sqrt{v_1 v_2}]/(1+\rho)$, dominates. An increase in correlations leads to a decrease in I_F^{mean} [46, 3] which is reflected in decreased discriminability between the stimuli (See panels c) and d) of Fig. 1). High values of the correlation coefficients have been used in Fig. 1 for easier visualization.

In contrast, correlation coding typically has a small effect in the case of two neurons, as the term I_F^{cov} is far smaller than I_F^{mean} . There are two reasons for this: The first holds only in the small correlation regime. Note that ρ enters I_F^{cov} at $\mathcal{O}(\rho^2)$, while it enters I_F^{mean} at $\mathcal{O}(\rho)$. The second holds for a larger range of correlation strengths: v'_i/v_i and ρ' are typically far smaller than $f'_i/\sqrt{v_i}$ and, as a result², $I_F^{\text{cov}} \ll I_F^{\text{mean}}$. Therefore, under fairly general assumptions, the dominant effect of correlations on Fisher information for cell pairs is via *correlation shaping* of I_F^{mean} .

Only close to perfect correlation, where $\rho \approx 1$, is the impact of correlation coding potentially significant. Assuming that $\rho' = O(1)$ as ρ approaches 1, and letting $\epsilon = 1 - \rho^2$, we have $I_F = 2\epsilon^{-2}(\rho')^2 + O(\epsilon^{-1})$. Therefore, when ρ is close to 1, most information about a stimulus can be carried by correlation changes. The balance between I_F^{mean} and I_F^{corr} close to perfect correlations strongly depends on the behavior of ρ' as ρ approaches 1. If ρ' approaches 0 as ρ approaches 1, as in [17], I_F^{mean} may continue to dominate.

²In detail: if responses are given by counting spikes over ~ 1 second, then typically f takes values substantially greater than 1. If firing is Poisson-like, then $v \approx f$. This leads to the stated dominance of f'/\sqrt{v} among these terms.

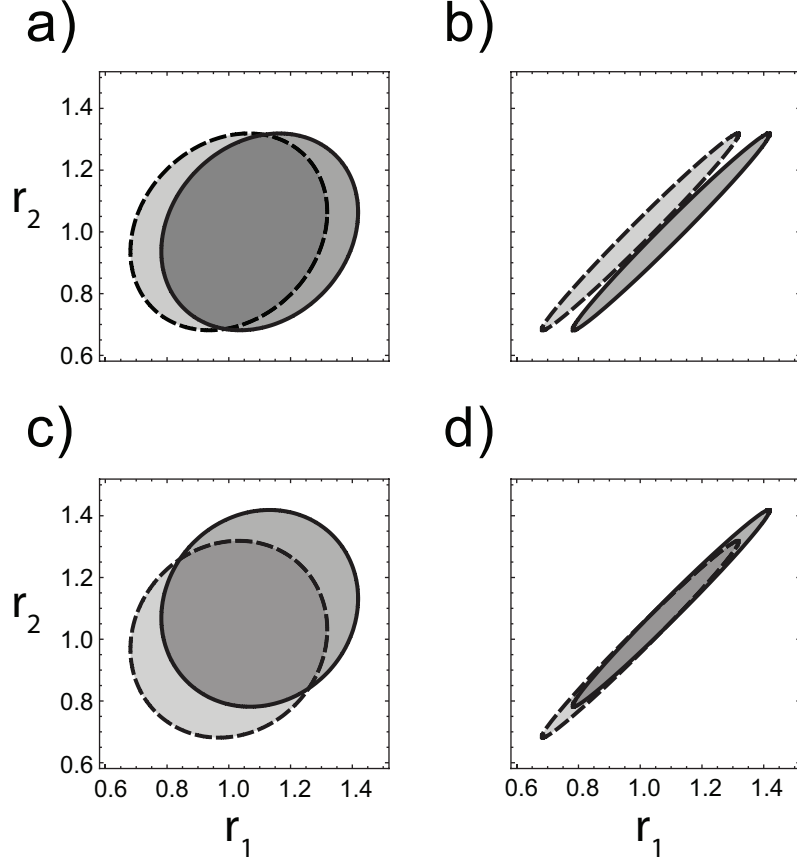


Figure 1: Illustration of correlation shaping for neuron pairs. Each panel shows 50% level curves of the joint density $p(r_1, r_2)$ in response to two nearby stimuli θ_A (dashed line) and θ_B (solid line). In all cases, $v_1 = v_2 = 1$. A change from stimulus θ_A to θ_B is assumed to affect only the f_i , so that $I_F^{\text{cov}} = 0$. The beneficial effect of correlations on I_F^{mean} (first term in Eq. (8)) is illustrated in panels a) and b). Here $f'_1(\theta_A) \neq f'_2(\theta_A)$, and increased correlations improve discriminability. In contrast, $f'_1(\theta_A) = f'_2(\theta_A)$ in panels c) and d), and increased correlations reduce discriminability. In panels a) and b): $f_1(\theta_A) = f_2(\theta_A) = 1$, while $f_1(\theta_B) = 1, f_2(\theta_B) = 1.1$. In panel a), $\rho = 0.2$, while in panel b), $\rho = 0.99$. In panels c) and d) $f_1(\theta_A) = f_2(\theta_A) = 1$, and $f_1(\theta_B) = f_2(\theta_B) = 1.1$. In panel c), $\rho = 0.1$, and in panel d), $\rho = 0.99$.

Fisher information in small populations Many of these observations extend to small populations of neurons with low correlations. Let

$$(I_F)_i^{\text{mean}} = \frac{(f'_i)^2}{v_i}, \quad (I_F)_i^{\text{var}} = \frac{1}{2} \left(\frac{v'_i}{v_i} \right)^2, \quad \text{and} \quad (I_F)_{i,j}^{\text{corr}} = \rho_{i,j} \rho'_{i,j} \left(\left[\frac{\rho'_{i,j}}{\rho_{i,j}} - \left(\frac{v'_i}{v_i} + \frac{v'_j}{v_j} \right) \right] \right).$$

We show in Appendix A that

$$I_F = \underbrace{\sum_i (I_F)_i^{\text{mean}} - \sum_{\substack{i,j \\ i \neq j}} \frac{f'_i f'_j \rho_{i,j}}{\sqrt{v_i v_j}} + \sum_{\substack{i,j,k \\ k \neq i,j}} \frac{f'_i f'_j \rho_{i,k} \rho_{k,j}}{\sqrt{v_i v_j}}}_{I_F^{\text{mean}}} + \underbrace{\sum_i (I_F)_i^{\text{var}} + \sum_{\substack{i,j \\ i \neq j}} \frac{\rho_{i,j}^2}{8} \left(\frac{v'_i}{v_i} - \frac{v'_j}{v_j} \right)^2 + \sum_{i < j} (I_F)_{i,j}^{\text{corr}}}_{I_F^{\text{cov}}} + O(\rho_{i,j}^3) \quad (9)$$

Here $(I_F)_i^{\text{mean}}$ and $(I_F)_i^{\text{var}}$ are $O(1)$, while $(I_F)_{i,j}^{\text{corr}}$ is $O(\rho_{i,j}^2)$. Therefore, I_F is a sum of contributions from individual neuron responses ($(I_F)_i^{\text{mean}}$ and $(I_F)_i^{\text{var}}$) and corrections of higher order in ρ due to correlations in the response.

Only the term $-\sum_{i,j,i \neq j} f'_i f'_j \rho_{i,j} / \sqrt{v_i v_j}$ in I_F^{mean} is of first order in ρ . This term therefore dominates the correction when correlations are small to intermediate. In this case, correlations between differently tuned neurons again increase I_F , and those between similarly tuned neurons decrease I_F . If correlations $\rho_{i,j}$ across the (small) population are stronger between neurons i and j for which f'_i and f'_j have opposite signs and weaker when these signs are the same, they increase I_F . This is in agreement with the two cell case discussed above, as well as previous results [6, 37, 3, 46].

Eq. (9) is general, under the assumption that the response follows a multivariate Gaussian distribution. However, the approximation starts breaking down when N exceeds $1/\rho_{i,j}$ (See Appendix A, and Fig. 6.)

4 Large populations with no spatial correlation decay

In general, for large populations it is difficult to obtain a closed form expression for I_F in terms of the variances, correlation coefficients and firing rates. Results are available under different simplifying assumptions that make the problem mathematically tractable [1, 48, 43]. In most cases it was assumed that correlation coefficients, $\rho_{i,j}$, are independent of the stimulus θ , so that $\rho'_{i,j} = 0$. In the following we refer to this as the Stimulus Independent (SI) case, and contrast it to the Stimulus Dependent (SD) case. The assumption that we make is that correlations between cell pairs, $\rho_{i,j}$, are given by Eq. (3), and that stimulus dependence of correlations, $S_{i,j}(\theta)$ takes the product form in Eq. (4).

In this section we let $c(\phi_i - \phi_j) = 1$. Therefore, the correlation structure is completely determined by the stimulus. In this case an analytical expression for \mathbf{Q}^{-1} and I_F can be found using the Sherman-Morrison Formula [29, p. 124]. We derive the exact expression for I_F for arbitrary population sizes N , arbitrary response characteristics $v_i(\theta)$, $f_i(\theta)$, and $s_i(\theta)$, as well as an approximation

valid for large populations, in Appendices B and C.

To give concrete examples of how stimulus dependence of correlations impacts I_F in large populations, in the remainder of the paper we further assume (as in, e.g., [41, 42, 46, 10]), that cell responses follow tuning curves that differ only by a phase shift, so that we can write

$$f_i(\theta) = f(\theta - \phi_i), \quad v_i(\theta) = v(\theta - \phi_i), \quad \text{and} \quad s_i(\theta) = s(\theta - \phi_i), \quad (10)$$

where $\theta, \phi_i \in [0, 2\pi)$. We take all functions to be periodic. The response, $f_i(\theta)$, is chosen so that neuron i responds preferentially (with maximum rate) to stimulus $\theta = \phi_i$, where ϕ_i is fixed. These are common assumptions that simplify the analysis considerably [46, 48]. Correlations are therefore determined by $\rho_{ij}(\theta) = s(\theta - \phi_i)s(\theta - \phi_j)$.

Assuming the neurons sample the stimulus space uniformly and sufficiently densely, we can use the continuum limit to approximate I_F . In this case, an arbitrary vector $\mathbf{a}(\theta)$ with components $a(\theta - \phi_i)$ tends to a function $a(\theta)$ of the stimulus θ . As we show in Appendix C, I_F can then be approximated as the sum of

$$I_F^{\text{mean}} \sim D\left(\frac{f'(\theta)}{\sqrt{v(\theta)}}, s(\theta)\right), \quad \text{and} \quad I_F^{\text{cov}} \sim \frac{N}{\pi} \int_0^{2\pi} \left(\frac{v'(\phi)}{2v(\phi)} - \frac{s'(\phi)s(\phi)}{1-s^2(\phi)}\right)^2 d\phi + D(G(\theta)s(\theta), s(\theta)), \quad (11)$$

where $G(\theta) = \left(s'(\theta) + \frac{v'(\theta)}{2v(\theta)}s(\theta)\right)$ and

$$D(a(\theta), s(\theta)) \approx \frac{N}{2\pi} \left[\int_0^{2\pi} \frac{a^2(\phi)}{1-s^2(\phi)} d\phi - \int_0^{2\pi} \frac{a(\phi)s(\phi)}{1-s^2(\phi)} d\phi \right] / \int_0^{2\pi} \frac{s^2(\phi)}{1-s^2(\phi)} d\phi. \quad (12)$$

By symmetry, neither I_F^{mean} , I_F^{cov} nor I_F depend on θ in the large population limit, since the response provides equal information about any stimulus. Therefore, we fix $\theta = \pi$ in the following, and write the firing rates, variances and correlations as functions of the neurons' preferred stimuli, ϕ . The correlation between two neurons with preferred stimuli ϕ and ϕ' will be denoted by $\rho(\phi, \phi')$, and $\rho(\phi) = \rho(\phi, \phi) = s^2(\phi)$ will be the correlation coefficient between two neurons with equal stimulus preference.

In the remainder of the paper, we make one final assumption: that the functions f , v , and s are even (i.e., symmetric around preferred orientations), as in, e.g., [46, 48] and many other studies.

Effects of stimulus-dependent correlations on I_F^{mean} : To illustrate how stimulus dependence of correlations can influence the information contained in the population response we first consider I_F^{mean} . Even when correlations are small, this stimulus dependence can have a strong effect via correlation shaping.

Since $f(\phi)$ and $v(\phi)$ are even, $f'(\phi)/\sqrt{v(\phi)}$ is odd. Therefore, setting $a(\phi) = f'(\phi)/\sqrt{v(\phi)}$, the second term in Eq. (12) vanishes, and

$$I_F^{\text{mean}} = \frac{N}{2\pi} \int_0^{2\pi} \frac{(f'(\phi))^2}{v(\phi)} \frac{1}{1-s^2(\phi)} d\phi. \quad (13)$$

Although I_F^{mean} is the average of the Fisher information $[f'_i]^2/v_i$ of *single* neurons, with a weighting factor, caution needs to be exercised when interpreting this result. Eq. (13) is the result of

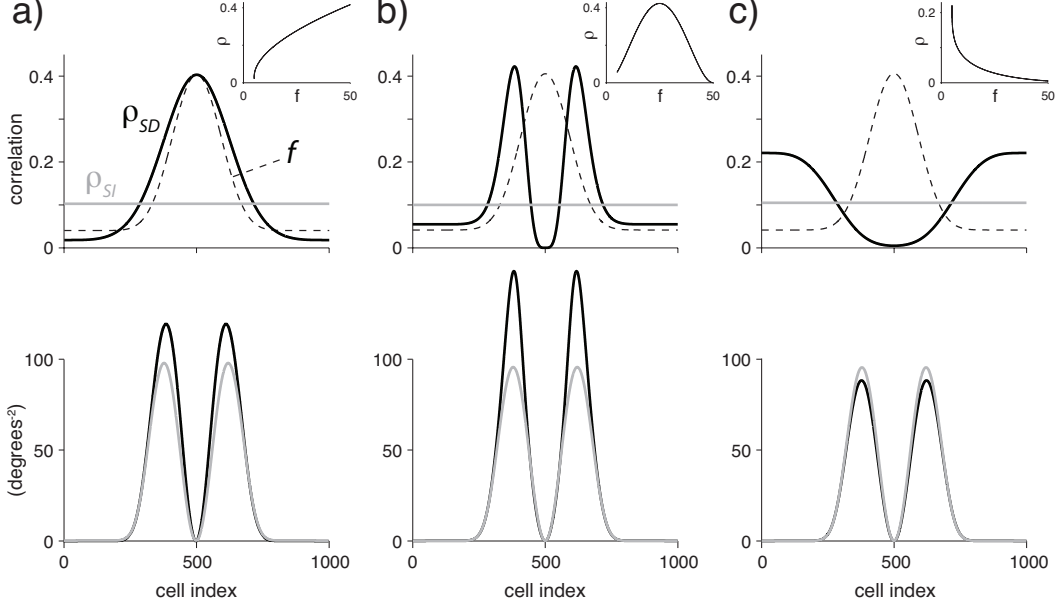


Figure 2: Examples of different correlation tuning curves and their impact on I_F^{mean} for large populations. Top panels show the correlation tuning curves, $\rho(\phi) = s^2(\phi)$ for the SD (black) and SI (gray) cases along with the (normalized) mean response $f(\phi)$ (dashed). Average correlations are matched to equal 0.1 in all cases. Insets illustrate the $\rho - f$ relationship for each choice of the correlation tuning. Bottom panels show the integrand of Eq. (13) for the SD (black) and SI (gray) cases. **a)** $\rho - f$ follows a concave increasing curve, and $\rho(\phi)$ shows a slightly broader tuning than $f(\phi)$ in the SD case, resulting in a substantial increase in I_F^{mean} with respect to the SI case (increase of $\sim 21\%$). **b)** $\rho - f$ is non-monotonic, and $\rho(\phi)$ is bimodal and matches $(f'(\phi))^2/v(\phi)$ in the SD case. This yields a larger enhancement of I_F^{mean} with respect to the SI case (increase $\sim 29\%$). **c)** Correlations that decrease with rate have a negative impact on I_F^{mean} (decrease of $\sim 7\%$ compared to the SI case). In all cases I_F^{mean} was computed in the large N limit using Eq. (11). Parameters: average correlation coefficient $\bar{s}^2 = 0.1$ in all cases (larger values, e.g. 0.2, will typically more than double the difference in I_F^{mean} between SD and SI cases). In all cases $f(\phi) = 5 + 45a^6(\phi)$ with $a(\phi) = 1/2(1 - \cos(\phi))$, and $v(\phi) = f(\phi)$ (Poisson). **(a)** $s(\phi) = k_\rho + b_\rho a^2(\phi)$ where $k_\rho = 0.135$ and $b_\rho = 0.5$; **(b)** $s(\phi) = 4r_{\text{max}}f(\theta)[f_{\text{max}} - f(\theta)]/f_{\text{max}}^2$ with $r_{\text{max}} = 0.65$ and $f_{\text{max}} = 50$; **(c)** $s(\phi) = k_\rho + b_\rho a^2(\phi)$ where $k_\rho = 0.47$ and $b_\rho = -0.4$. (See Appendix E.)

simplifying an expression derived from all pairwise interactions across the population.

In the SI case, each $s_i(\theta)$ is independent of the stimulus, and $s(\phi)$ is therefore constant across the population: $s(\phi) = \bar{s}$. We focus on comparisons between SI and SD cases matched to have the *same* average correlation coefficient across the population. *We therefore assess the effects of the stimulus-dependence of correlation, as opposed to the level of correlations.* Specifically, we ensure that the average correlation coefficient across the population in the SD case, $(4\pi^2)^{-1} \int_0^{2\pi} \int_0^{2\pi} s(\phi_1)s(\phi_2) d\phi_1 d\phi_2$, equals that in the SI case by setting $\bar{s} = 1/(2\pi) \int_0^{2\pi} s(\phi)d\phi$. Examples of typical matched correlation matrices, ρ_{ij} , in the SD and SI cases, are shown in the right hand column of Fig. 3.

Panels a) and b) of Fig. 2 illustrate how correlation shaping may increase I_F^{mean} in the SD case over the SI case. In each, stimulus-dependence of correlations arises from a different relationship between stimulus-induced firing rate and correlation (see insets). In a), $\rho(\phi)$ increases with $f(\phi)$, as in [17] and certain regimes in [8, 26, 22]. In b), $\rho(\phi)$ first increases with $f(\phi)$, and then decreases, as in feed-forward networks with refractory effects [45]. Importantly, for both panels a) and b), correlations are high between neurons that individually carry most information about the stimulus (i.e., between neurons with large values of $(f'(\phi))^2/v(\phi)$). Therefore, the weighting factor $1/(1 - s^2(\phi))$ assigns a greater contribution of these more-informative cells to the weighted average in Eq. (13) for the SD case, leading to the increase in I_F^{mean} .

On the other hand, panel c) of Fig. 2 illustrates a case in which correlations decrease with firing rates, as observed in [2]. As a result, correlations between the most informative neurons are smaller than average, and correlation shaping negatively impacts I_F . We note that in all panels maximum pairwise correlations satisfy $\rho_{\text{max}} \lesssim 0.45$, within the range typically reported (e.g., [23, 34, 49]). Increasing this maximum, without changing the mean correlation, can make these correlation shaping effects more pronounced.

A different way of seeing how I_F^{mean} can be greater in the SD than the SI case is given in Fig. 3a. Here, I_F^{mean} and I_F^{cov} are computed numerically, and plotted as a function of the population size N , for both the SD and SI cases that correspond to the example of correlations increasing with rate (Fig. 2a). Note that I_F^{mean} dominates I_F^{cov} over a wide range of N and that the total Fisher information, not just I_F^{mean} , is greater in the SD vs. SI case. Moreover, the continuum limit given in Eq. (13) appears valid even for moderate population sizes.

Care needs to be taken when trying to intuitively understand these population-level effects of stimulus-dependent correlations on I_F^{mean} by invoking the case of two neurons studied in Section 3. Consider the case of correlations increasing with firing rate (Figs. 3a, 4a). As noted in the discussion of Eq. (8), an increase in correlations between two similarly tuned neurons will typically have a negative impact on I_F^{mean} , due to the dominance of the second term of I_F^{mean} in Eq. (8). On the other hand, Eq. (13) shows that increasing correlations between the most informative neurons in a large population, regardless of the similarity of their tuning, has a positive impact. The two results are not contradictory. Consider the pairwise sum of the two-neuron I_F^{mean} from Eq. (8) over *all neuron pairs* in the population. Note that the second term of I_F^{mean} in Eq. (8) can be expected to be matched with one of equal and opposite sign in such a sum, if the tuning curves are symmetric, and correlations depend only on firing rate. Therefore, the typically-dominant second term cancels, and it is the *first* term in Eq. (8), always positively impacted by the presence of correlation, that remains. Moreover, examination of this first term in Eq. (8) does show similarity with Eq. (13): in both cases, assigning largest correlations $\rho_{i,j}$ or $s(\phi, \phi')$ to most-informative neurons will yield the greatest total value of I_F^{mean} .

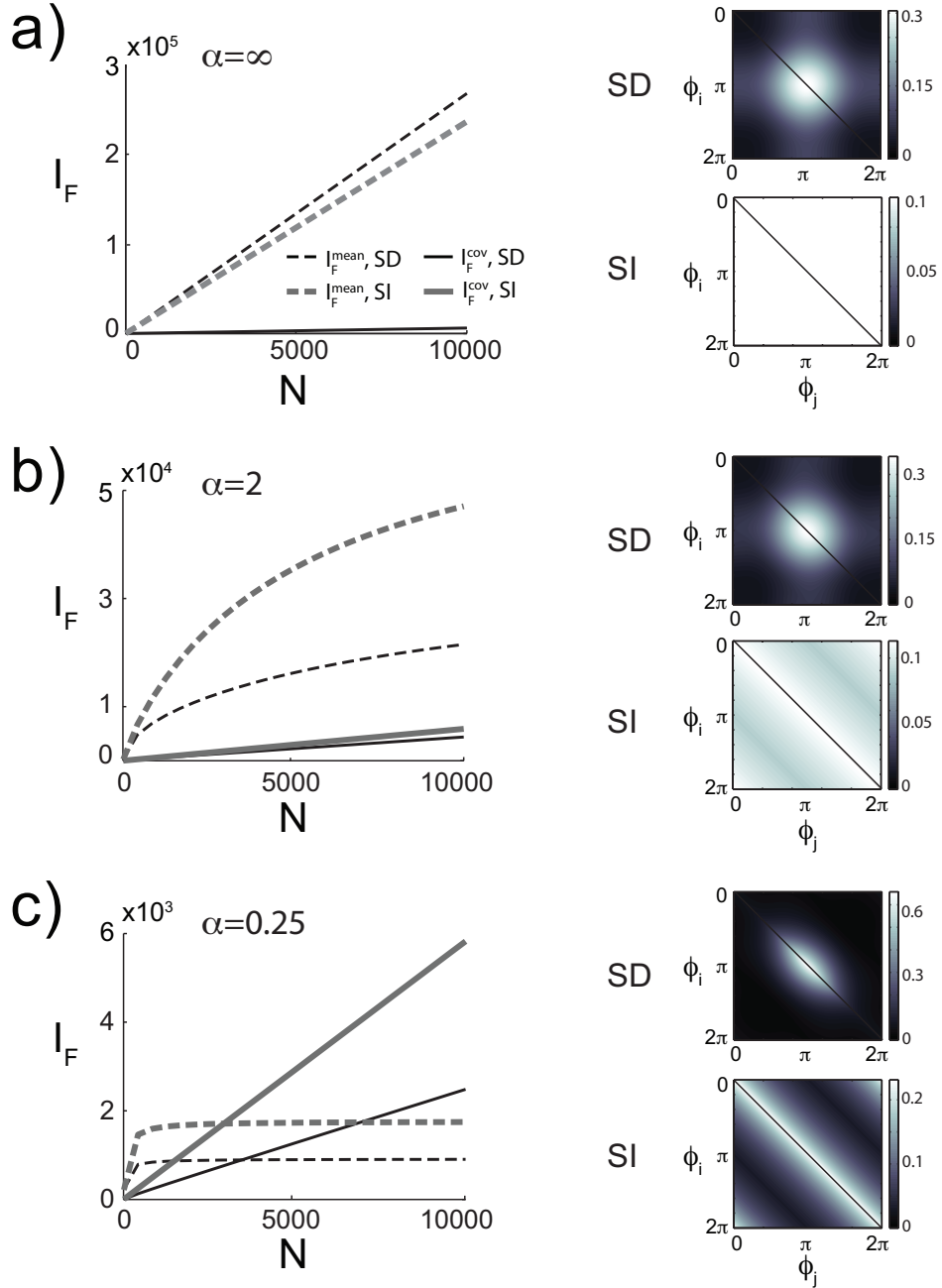


Figure 3: I_F^{mean} and I_F^{cov} as a function of population size N , for matched SD and SI correlation cases and various correlation decay lengthscales. Here, correlation is assumed to increase with firing rate, as in Fig. 2a). The coefficients k_ρ and b_ρ defining $s(\phi) = k_\rho + b_\rho a^2(\phi)$ are chosen to keep the average correlation coefficients over the population equal to 0.1 (See Appendix E). The corresponding correlation matrices, $\rho_{i,j}$, for the SD and SI cases are also shown (on-diagonal terms are set to 0 in these plots).

Fig. 4a) shows that this cancellation argument, while not *directly* applicable, is at least analogous to what happens when computing I_F^{mean} for the large population via the complete expression (11). The sum of the terms $f'_i f'_j Q_{i,j}^{-1}$ defines the linear Fisher information, $I_F^{\text{mean}} = \sum_{i,j} f'_i f'_j Q_{i,j}^{-1}$ (see Eq. (6)). Under the present symmetry assumptions, the off-diagonal terms cancel, and only the diagonal terms contribute to the sum. In Appendix C we show that $Q_{i,i}^{-1} = [v_i(1 - s_i^2)]^{-1}$, in agreement with the remaining term in Eq. (13).

These observations are robust to the presence of weak asymmetry in the functions f , v , and s . For instance, when the tuning curve $f(\theta)$ is a sum of a symmetric and small asymmetric part, $f_{\text{sym}}(\theta) + \epsilon f_{\text{asym}}(\theta)$, an examination of Eq. (12) shows that the impact of the asymmetry on $I_F^{\text{mean}} = D(\frac{f'(\theta)}{\sqrt{v(\theta)}}, s(\theta))$ is of order $O(\epsilon N)$, while I_F^{mean} is $O(N)$. However, we show in the next section that the large population limit can be changed significantly when $c(\phi_i - \phi_j)$ is not constant.

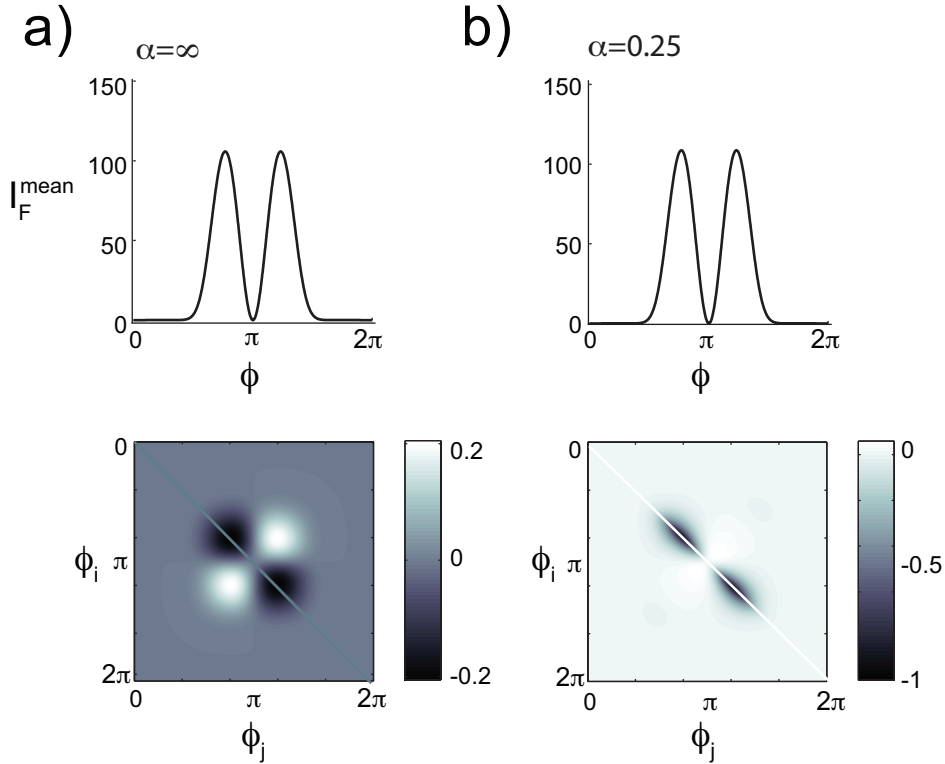


Figure 4: Plots of the matrix $f'_i f'_j Q_{i,j}^{-1}$ whose double sum determines I_F^{mean} . **a)** no spatial correlation decay, and **b)** spatial decay with $\alpha = 0.25$. Top: on-diagonal terms of matrix. Bottom: off-diagonal terms (with on-diagonal values set to 0 for ease of visualization).

Effects of stimulus-dependent correlations on I_F^{cov} : Having discussed I_F^{mean} , we now turn to the impact on I_F^{cov} of the stimulus-dependence of correlations. In Appendix D we show that this

impact is negligible for small to intermediate correlations, and that

$$I_F^{\text{cov}} \approx \frac{N}{2\pi} \int_0^{2\pi} \frac{v(\phi)}{2v'(\phi)} d\phi. \quad (14)$$

Moreover, as discussed in Section 3, values of $v(\phi)2v'(\phi)$ are typically smaller in magnitude than values of $\frac{(f'(\phi))^2}{v(\phi)}$. Therefore, for small to intermediate correlations the major contribution of the stimulus-dependence of correlations comes from I_F^{mean} rather than I_F^{cov} . This agrees with the case of two cells (Sec. 3). Asymptotic estimates of the integrals in I_F^{cov} show that this remains true even for correlation coefficients *close to one*. The dominance of I_F^{mean} over I_F^{cov} is apparent in Fig. 3a). As we show in the next section, however, that this dominance may no longer hold in the presence of spatial decay of correlations [46, 43].

Summary of Sec. 4: Stimulus-dependence may shape the structure of correlations so that neurons that are most informative about the stimulus presented are most highly correlated. This can lead to an increase in overall information. This is possible even when the average correlations across the population are low, but not when correlations are fixed, or if all neurons have identical mean responses.

5 Effects of correlation stimulus dependence in the presence of spatial decay

In this section we examine how stimulus-dependent correlations affect I_F in the presence of spatial correlation decay. We again assume that correlations and rates are described by Eqs. (3–4), but we now assume that

$$c(\phi_i - \phi_j) = C \exp \left[-\frac{|\phi_i - \phi_j|}{\alpha} \right].$$

The constant α determines the spatial range of correlations, while C was chosen so that the average correlation across the population $\langle \rho_{i,j} \rangle$ remains constant as other parameters are varied (for details see Appendix E). As an exact expression for the inverse of the covariance matrix is difficult to obtain, we study this case numerically, and give an intuitive explanation of the results.

Effect of correlation shaping on I_F^{mean} : When $\alpha = \infty$, there is no spatial decay, and we are in the situation discussed in the previous section: I_F is typically dominated by I_F^{mean} , which grows linearly with population size N (Fig. 3a). However, for finite values of α , I_F^{mean} generally *saturates* with increasing N (Fig. 3b,c). This agrees with earlier findings for stimulus-independent correlations [43, 44].

Additionally, effects of stimulus-dependence in correlations on I_F^{mean} can be *reversed* for finite values of α . For example, assume that $s_i(\phi)$ increases with the firing rate, as in Fig. 2a). When $\alpha = \infty$, stimulus-dependence of correlations increases I_F^{mean} (Fig. 3a). However, for finite α , this stimulus dependence has a negative impact on I_F^{mean} (Fig. 3b,c).

Intuitively, this may be due to spatial correlation decay reducing correlations between neurons with *differing* stimulus preferences. The negative impact of correlations between similarly tuned neurons on I_F is no longer balanced by the positive impact on differently tuned neurons. Indeed, the stronger the spatial decay of correlations, the more this balance is broken. Therefore, the

cancellation arguments presented in the previous section no longer hold – compare Fig. 3b) and c) – and it is no longer the case that simply increasing correlations for more-informative neurons will increase I_F^{mean} . Instead, correlation structures that increase correlation for similarly vs. differently tuned neurons can again be expected to decrease I_F^{mean} . Figure 4 shows that this is the precisely the effect of the SD vs. SI correlation structures.

As a second example, assume that correlations decrease, rather than increase, with firing rate, as in Fig. 2b. In this case, correlations between similarly tuned, strongly responding neurons are decreased. As expected from the arguments above, stimulus-dependent correlations then increase I_F^{mean} over its value in the stimulus-independent case. Moreover, absolute levels of I_F increase twofold compared to the analogous case where correlations increase with rate (compare Fig. 3c and Fig. 5a).

However, in all of these cases, note that levels of I_F are lower in the presence of correlation decay for *both* SD and SI cases. We now mention one way in which this can be mitigated. As illustrated in Fig. 5b), we increase the number of areas or subpopulations that respond strongly to a given stimulus. The response of each cell still follows a unimodal tuning curve, as above. However, the entire population has a number of cells at different spatial locations that share the same stimulus preference. Therefore, cells in different subpopulations are only weakly correlated and can be thought of as members of different, nearly independent populations. As Fig. 5b) shows, this boosts overall levels of I_F^{mean} , while maintaining the benefit of stimulus-dependence in correlations within individual subpopulations.

In sum, the spatial decay of correlations has a strong negative effect on linear Fisher information I_F^{mean} . If correlations depend on stimuli via an increasing relationship with firing rate, this effect can be accentuated, with levels of I_F^{mean} decreasing by a further factor of two for SD vs. SI cases. However, the opposite effect occurs if correlations decrease with rate: stimulus-dependence can then approximately double I_F^{mean} .

Effect of correlation coding on I_F^{cov} : For large populations, Figs. 3, 5 show that information can be carried predominantly by I_F^{cov} , and this dominance is more pronounced as the correlation lengthscale α decreases. This agrees with earlier findings [46, 43]. Moreover, we see that the effects of stimulus dependence of correlations on I_F^{cov} have the same “sign” as those on I_F^{mean} . Specifically, when correlations increase with rate, as in Fig. 3, both I_F^{mean} and I_F^{cov} are lower in the SD than in the SI cases, for finite values of correlation length α . Also, when correlations decrease with rate, as in Fig. 5, corresponding values of both I_F^{mean} and I_F^{cov} are higher for the SD than the SI case.

The effects of stimulus dependence on the (dominant) I_F^{cov} terms can be attributed to *correlation coding*. In detail, the contribution of $\rho'_{ij}(\theta)$ terms to I_F^{cov} can be isolated numerically by simply computing I_F^{cov} twice: once with these terms at the nonzero values expected from stimulus dependence, and once after “artificially” setting all of these terms equal to zero. The difference is the contribution to I_F attributable directly to changes in correlation with the stimulus (i.e., correlation coding, as opposed to the correlation shaping effects that have been the focus of much of the previous discussion). Our calculations (not shown) indicate that almost the entire increase, or decrease, of I_F^{cov} in the SD relative to the SI cases is due to this correlation coding.

Remark 1: More heterogeneous populations of neurons have been shown to yield higher values of Fisher information in some cases [44, 12]. We modeled such heterogeneity by randomly and independently jittering the tuning curves of the neurons, while preserving the expected correlation

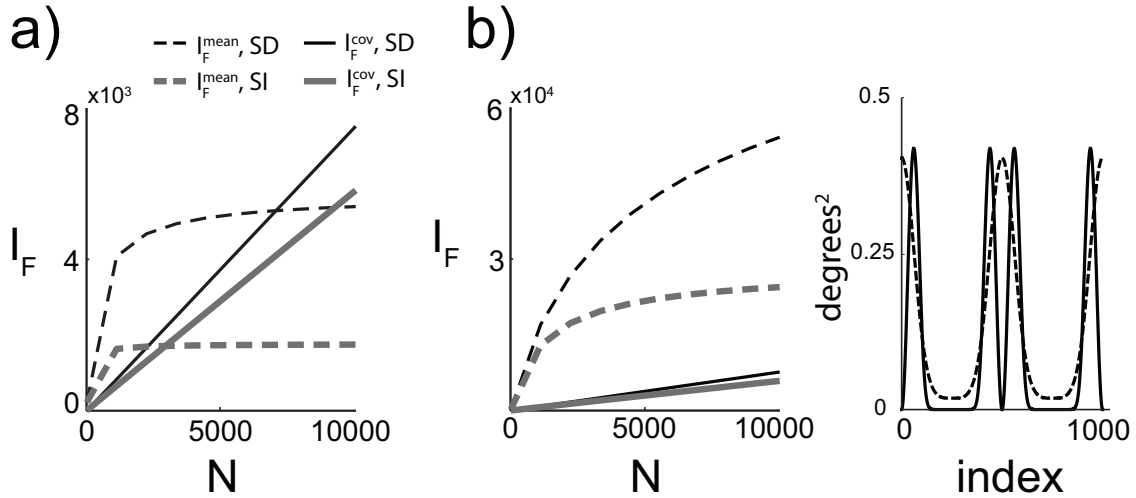


Figure 5: Examples where the Fisher information is larger in the SD than the SI case, despite strong correlation decay $\alpha = 0.25$. In each case (as in all of Figs. 2-6), $s(\phi)$ is set so that the average correlation coefficient ρ across the population is 0.1. **a)** Correlations *decrease* with firing rate, as in Fig. 2c). **b)** The response of a population with two subpopulations each tuned to the stimulus. In the right panel, as in Fig. 2, $(f'(\phi))^2/v(\phi)$ is scaled and represented by the solid line, while $\rho(\phi) = s(\phi)^2$ is represented by the dotted line. The effects of spatial correlation decay are not shown. The response of each cell in the population follows a unimodal tuning curve; however, there are two sets of cells at different spatial locations, that share the same stimulus preference. The left panel shows the effect of this arrangement on the Fisher information. Other parameters are as in Fig. 3.

between pairs. Perturbing the different tuning curves by 10% had a relatively small impact on the present results. Specifically, I_F terms still increased (or decreased) in the same SD vs SI cases. Moreover, although I_F^{mean} does not necessarily saturate, for small perturbations I_F^{cov} still dominates even at large population sizes.

Remark 2: As discussed in Section 2, it has been observed that correlations between neuronal responses decrease with the difference between their preferred stimuli [49, 28]. This effect can also follow from stimulus-dependence of correlations: When correlations increase with firing rate, two neurons that both respond strongly to similar stimuli will be more correlated than those of neurons whose preferences differ. As neurons with similar preferences in stimuli can be expected to be physically closer in the cortex, stimulus dependence can result in correlations that decay with physical distance [45]. This is quite different from the case where physically distant cells are less correlated due to a smaller overlap in their inputs. With stimulus-dependence of correlations, two distant cells, one or both of which are responding strongly, may be more correlated than two nearby cells that are both responding weakly (see Fig. 3).

6 Discussion

Correlations in the neural response have the potential to both positively and negatively impact the ability of a population to carry information about stimuli. Intuitively, correlated fluctuations imply a common component in the response noise of different neurons. Similarly tuned neurons may provide redundant information, as the common noise component cannot be directly averaged away [24, 9, 49]. However, it is also possible that noise can be removed by taking differences between neural responses [1]. The net effect of correlations on population level information therefore depends on the balance among different effects.

We considered neuronal populations with stimulus-dependent correlations and discussed two ways in which such stimulus dependence influences Fisher information. The first, correlation coding, refers to the information directly carried by changes in correlation structure in response to stimuli. The second, correlation shaping, refers to the impact of stimulus dependence on information carried by the mean and variance of neural responses. In different cases, we derived expressions for the Fisher information that isolate correlation shaping and correlation coding effects: For cell pairs, and small-to-intermediate populations Eqs. (8), (9) are valid for general correlation structures. For correlations with product structure, $\rho_{ij}(\theta) = s_i(\theta)s_j(\theta)$, expressions are derived for populations of arbitrary size N , with simplifications in the continuum limit $N \rightarrow \infty$ (Eqs. (13) and (14)).

These expressions allow us to make a number of general observations. For typical firing regimes, we find that the effects of correlation shaping dominate over those of correlation coding for pairs of neurons or small populations with weak-to-moderate correlations, with most information being carried by I_F^{mean} . Correlation coding only becomes significant for strong correlations. However, for large populations the answer is different. Without spatial decay of correlations, correlation shaping and I_F^{mean} dominate (cf. [43, 44]) regardless of correlation strength. However, correlation coding and I_F^{cov} become important in the presence of decay.

Additionally, for pairs of neurons or small populations with weak correlations, correlated responses between similarly tuned neurons typically decrease I_F^{mean} , while correlations between oppositely tuned neurons increase I_F^{mean} , as has been shown in related settings (cf. [6, 37, 3, 46]).

However, for large populations with symmetric and uniformly distributed tuning curves, the situation may be quite different. For correlations with product structure and without spatial decay, $\rho_{ij}(\theta) = s_i(\theta)s_j(\theta)$, correlations between the “most-informative” neurons (those with largest $f'_i(\theta)/\sqrt{v_i(\theta)}$) have the greatest impact on I_F^{mean} , regardless of similarity of tuning. Some forms of stimulus dependence can increase these correlations, providing a boost to the Fisher information; others decrease these correlations and hence the Fisher information. Interestingly, in the presence of spatial decay of correlations, these effects of stimulus dependence on Fisher information are typically reversed. We note one interpretation: since spatial decay tends to decrease Fisher information, the correct stimulus dependence of correlations can counterbalance this effect.

What biological mechanisms could underly different patterns of stimulus-dependent correlation? One is the co-tuning of correlation and response rate that has been observed in feed-forward networks [17, 45]. More complex network effects could be behind the decreasing trend of correlation with rates seen in [2]. Moreover, stimulus-dependent adaptation of correlations has been observed in the visual cortex [27, 20, 23]. Our study points to the potentially distinct impacts of the mechanisms on population codes.

Fisher information is only one of the possible metrics that can be used to quantify the impact of correlations. However, its close connection with stimulus discriminability [16], relative ease of computation compared to other metrics, and recent use in experimental settings [23, 6] make it a good starting point. Future work will extend our study of the impact of correlation stimulus dependence to other metrics, such as mutual information, adding to results of [30, 32].

Another important question for future work comes from decoding: how can information encoded in correlation changes be read out? For cases in which information is dominated by I_F^{mean} terms, a linear readout will suffice; however, when I_F^{cov} dominates, as for large populations with distance-dependent decay of correlations, nonlinear schemes are required [43].

Acknowledgments We thank Bruno Averbeck, Jeff Beck, and Adam Kohn for their insights and helpful comments and suggestions. E. S.-B. holds a Career Award at the Scientific Interface from the Burroughs-Wellcome Fund. This research was also supported NIH grant DC005787-01A1 (J. R.), a Texas ARP/ATP, and NSF grant DMS-0604429 to K.J., and NSF grant DMS-0817649 to B. D., K.J., and E. S.-B.

A Fisher information for small populations with small correlations

The appendices contain a number of exact expressions and approximations of the Fisher information for both intermediate and large populations. These results should be useful in the further analysis of the impact of correlations in settings similar and distinct from those studied here.

The approximation in (9) is obtained from the assumption $|\rho_{i,j}| \ll 1$. Defining $\epsilon\tilde{\rho}_{i,j} = \rho_{i,j}$, we can write

$$Q_{i,j} = \delta_{i,j}v_i + \epsilon(1 - \delta_{i,j})\tilde{\rho}_{i,j}\sqrt{v_iv_j}.$$

Therefore \mathbf{Q} is a perturbation of a diagonal matrix \mathbf{R} with entries $R_{i,j} = \delta_{i,j}v_i(x)$, and the perturbation $\epsilon\mathbf{S}$ where $S_{i,j} = (1 - \delta_{i,j})\tilde{\rho}_{i,j}(x)\sqrt{v_i(x)v_j(x)}$. We can now use the standard matrix perturbation

result (see also [48, 19])

$$\begin{aligned}
\mathbf{Q}^{-1} &= [\mathbf{R}(\mathbf{I} + \epsilon \mathbf{R}^{-1} \mathbf{S})]^{-1} = (\mathbf{I} + \epsilon \mathbf{R}^{-1} \mathbf{S})^{-1} \mathbf{R}^{-1} \\
&= \left[\sum_{i=0}^{\infty} (-\epsilon \mathbf{R}^{-1} \mathbf{S})^i \right] \mathbf{R}^{-1} \\
&= \mathbf{R}^{-1} - \epsilon \mathbf{R}^{-1} \mathbf{S} \mathbf{R}^{-1} + \epsilon \mathbf{R}^{-1} \mathbf{S} \mathbf{R}^{-1} \mathbf{S} \mathbf{R}^{-1} + (\epsilon^3).
\end{aligned} \tag{15}$$

The equality on the second line holds whenever $\|\epsilon \mathbf{R}^{-1} \mathbf{S}\| < 1$ for a norm $\|\cdot\|$ which is consistent with itself [19, Lemma 2.1]. Using (15), we obtain

$$Q_{i,j}^{-1} = \delta_{i,j} \frac{1}{v_i} - \epsilon (1 - \delta_{i,j}) \frac{\tilde{\rho}_{i,j}}{\sqrt{v_i v_j}} + \epsilon^2 \sum_{\substack{k \\ k \neq i,j}} \frac{\tilde{\rho}_{i,k} \tilde{\rho}_{k,j}}{\sqrt{v_i v_j}}. \tag{16}$$

Using this equation, the first term in the expression for I_F , $\mathbf{f}^T \mathbf{Q}^{-1} \mathbf{f}$, can be computed directly, to obtain the expression on the first line of (9). The second term, $\text{Tr}[(\mathbf{Q}' \mathbf{Q}^{-1})^2]/2$, can be computed similarly, through a lengthier computation. This computation can be simplified using the observations in the next section. This gives Eq. (9), keeping terms up to second order.

The convergence of the sum on the second line of (15) is not guaranteed if $\|\epsilon \mathbf{R}^{-1} \mathbf{S}\| > 1$. This implies that for fixed ϵ , the approximation (16) will break down for sufficiently large N (typically about when $N > 1/\epsilon$).

B General expression for I_F in the product case

In this section we use the Sherman-Morrison Formula [29, p. 124] to derive a general expression for the Fisher information in the product case. Let

$$\mathcal{S} = \sum_{j=1}^N \frac{s_j^2}{(1 - s_j^2)}. \tag{17}$$

Then

$$Q_{i,j}^{-1} = \begin{cases} \frac{1}{v_i(1 - s_i^2)} \left(1 - \frac{s_i^2}{(1 + \mathcal{S})(1 - s_i^2)} \right) & \text{if } i = j \\ -\frac{s_i s_j}{\sqrt{v_i v_j} (1 + \mathcal{S})(1 - s_i^2)(1 - s_j^2)} & \text{if } i \neq j. \end{cases} \tag{18}$$

Using this equation we can obtain a compact expression for I_F . The term resulting from changes in the mean number of spikes as the stimulus varies is given directly from definition (7) as

$$I_F^{mean}(x) = \sum_{i,j=1}^N f'_i f'_j Q_{i,j}^{-1}. \tag{19}$$

The contribution to I_F due to changes in the covariance, given by $I_F^{cov} = \text{Tr}[(\mathbf{Q}' \mathbf{Q}^{-1})^2]/2$, can

be expressed compactly by introducing

$$R_i = \frac{d}{dx} \ln s_i = \frac{s'_i}{s_i}, \quad \text{and} \quad Z_i = \frac{d}{dx} \ln(s_i \sqrt{v_i}) = \frac{s'_i}{s_i} + \frac{1}{2} \frac{v'_i}{v_i}. \quad (20)$$

Note that when $\rho_{i,j}$ have the form given in Eq. (3), $c(\phi_i - \phi_j) = 1$, and the stimulus dependence of correlations, $S_{i,j}(\theta)$ takes the product form in Eq. (4) If , we can write

$$Q'_{i,j} = (Z_i + Z_j - 2\delta_{i,j} R_i) Q_{i,j},$$

where Z_i and R_i are defined in (20). Following this observation, we can follow the computations in [48, Appendix A], to obtain

$$\frac{\text{Tr}[(\mathbf{Q}'\mathbf{Q}^{-1})^2]}{2} = \sum_{k=1}^N Z_k^2 + \sum_{k,l=1}^N Q_{k,l} Z_k Z_l Q_{l,k}^{-1} - 4 \sum_{k=1}^N Q_{k,k} Z_k R_k Q_{k,k}^{-1} + 2 \sum_{k,l=1}^N Q_{k,k} Q_{l,l} R_k R_l Q_{k,l}^{-1} Q_{l,k}^{-1}.$$

Observing that \mathbf{Q}^{-1} is self-adjoint, we obtain

$$\begin{aligned} I_F^{\text{cov}} &= \sum_{i=1}^N (Z_i)^2 \left[1 + Q_{i,i}^{-1} v_i (1 - s_i^2) \right] + \sum_{i,j}^N Z_i Z_j s_i s_j \sqrt{v_i v_j} Q_{i,j}^{-1} \\ &+ 2 \sum_{i,j}^N R_i R_j \left[\sqrt{v_i v_j} Q_{i,j}^{-1} \right]^2 - 4 \sum_{i=1}^N Z_i R_i v_i Q_{i,i}^{-1}. \end{aligned} \quad (21)$$

Therefore, I_F is the sum of (19) and (21).

The contribution to I_F due to only changes in the variances can be obtained from Equation (21) by setting $R_i = 0$ and replacing Z_i by $v'_i/(2v_i)$, so that

$$I_F^{\text{var}} = \sum_{i=1}^N \left(\frac{v'_i}{2v_i} \right)^2 \left[1 + Q_{i,i}^{-1} v_i (1 - s_i^2) \right] + \sum_{i,j}^N \frac{v'_i v'_j s_i s_j}{4\sqrt{v_i v_j}} Q_{i,j}^{-1}. \quad (22)$$

The contribution due to correlation stimulus dependence is therefore

$$I_F^{\text{corr}} = I_F^{\text{cov}} - I_F^{\text{var}}.$$

C Asymptotic results

The expression for I_F derived in Appendix B can be simplified considerably for large cell populations. If N is large and $0 < \epsilon < s_i < 1 - \delta$ for some $\epsilon, \delta > 0$, then $\mathcal{S} = O(N)$, where \mathcal{S} is defined in (17). The assumptions on s_i are not essential, but make the derivation of the asymptotic expressions easier.

Keeping only the leading order terms in (18) we can write

$$Q_{i,j}^{-1} \approx \begin{cases} \frac{1}{v_i(1-s_i^2)} & \text{if } i = j \\ -\frac{s_i s_j}{\sqrt{v_i v_j} \mathcal{S}(1-s_i^2)(1-s_j^2)} & \text{if } i \neq j. \end{cases} \quad (23)$$

To obtain the asymptotic value of I_F given in (26) from Eqs. (19) and (21), first note that $\mathcal{S} = O(N)$. Therefore, for large N ,

$$\sum_{i,j}^N R_i R_j \left[\sqrt{v_i v_j} Q_{i,j}^{-1} \right]^2 \sim \sum_i^N \left[R_i v_i Q_{i,i}^{-1} \right]^2.$$

Using this observation together with the asymptotic value of $Q_{i,i}^{-1}$ given in (23), the first, and last two sums on the right hand side of (21) behave asymptotically as

$$\sum_{i=1}^N (Z_i)^2 \left[1 + Q_{i,i}^{-1} v_i (1-s_i^2) \right] + 2 \sum_{i,j}^N R_i R_j \left[\sqrt{v_i v_j} Q_{i,j}^{-1} \right]^2 - 4 \sum_{i=1}^N Z_i R_i v_i Q_{i,i}^{-1} \sim 2 \sum_{i=1}^N \left(Z_i - \frac{R_i}{1-s_i^2} \right)^2.$$

By a slight abuse of notation define the weighted average of the entries in the vector \mathbf{a} over the population as

$$\frac{1}{N} \sum_i^N \frac{a_i^2}{1-s_i^2} = \left\langle \frac{\mathbf{a}^2}{\mathbf{1}-\mathbf{s}^2} \right\rangle,$$

and let

$$D(\mathbf{a}, \mathbf{s}) \stackrel{\text{def}}{=} N \left[\left\langle \frac{\mathbf{a}^2}{\mathbf{1}-\mathbf{s}^2} \right\rangle - \left\langle \frac{\mathbf{a}\mathbf{s}}{\mathbf{1}-\mathbf{s}^2} \right\rangle^2 / \left\langle \frac{\mathbf{s}^2}{\mathbf{1}-\mathbf{s}^2} \right\rangle \right]. \quad (24)$$

Then the observations above can be combined with

$$\begin{aligned} \sum_{i,j}^N a_i a_j \sqrt{v_i v_j} Q_{i,j}^{-1} &\approx \left[\left(\sum_i^N \frac{a_i^2}{1-s_i^2} \right) \left(\sum_j^N \frac{s_j^2}{1-s_j^2} \right) - \left(\sum_i^N \frac{a_i s_i}{1-s_i^2} \right)^2 \right] / \left(\sum_j^N \frac{s_j^2}{1-s_j^2} \right) \\ &= N \left[\left\langle \frac{\mathbf{a}^2}{\mathbf{1}-\mathbf{s}^2} \right\rangle \left\langle \frac{\mathbf{s}^2}{\mathbf{1}-\mathbf{s}^2} \right\rangle - \left\langle \frac{\mathbf{a}\mathbf{s}}{\mathbf{1}-\mathbf{s}^2} \right\rangle^2 \right] / \left\langle \frac{\mathbf{s}^2}{\mathbf{1}-\mathbf{s}^2} \right\rangle \\ &\stackrel{\text{def}}{=} D(\mathbf{a}, \mathbf{s}). \end{aligned} \quad (25)$$

applied to the term I_F^{mean} and the second sum on the right hand side of (21), gives

$$I_F^{\text{mean}}(x) \sim D\left(\frac{\mathbf{f}'}{\sqrt{\mathbf{v}}}, \mathbf{s}\right), \quad \text{and} \quad I_F^{\text{cov}}(x) \sim 2 \sum_i^N \left(\frac{v'_i}{2v_i} - \frac{s'_i s_i}{1-s_i^2} \right)^2 + D(\mathbf{G}\mathbf{s}, \mathbf{s}), \quad (26)$$

where $G_i = \frac{d}{dx} \ln(s_i \sqrt{v_i}) = s'_i/s_i + \frac{1}{2} v'_i/v_i$. As before, I_F^{mean} corresponds to the linear Fisher information.

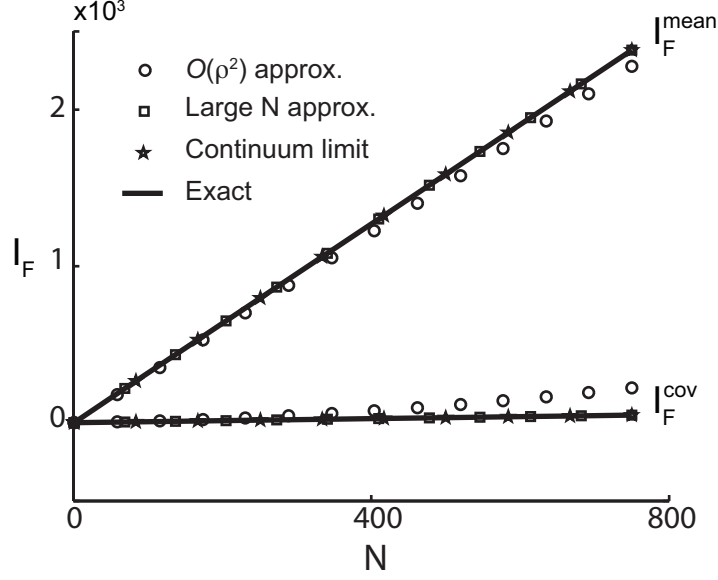


Figure 6: Values of I_F^{mean} and I_F^{cov} from: *i*) approximations for small ρ , valid for intermediate population sizes N , given by Eq. (9) *ii*) the “exact” value obtained by numerically inverting the correlation matrix \mathbf{Q} , and using Eqs. (6–7), *iii*) the large N approximation given by Eq. (26), and *iv*) the continuum limit given by Eq. (11–12). Here, $f(\phi) = 5 + 45a(\phi)$ with $a(\phi) = 1/2(1 + \cos(\phi))$, and $v(\phi) = f(\phi)$ (as for Poisson variability). Additionally, $s(\phi) = 0.2 + 0.5a(\phi)$. Other parameter choices give similar results (not shown).

The Cauchy inequality can be applied directly to show that

$$\left\langle \frac{\mathbf{a}^2}{1 - \mathbf{s}^2} \right\rangle \left\langle \frac{\mathbf{s}^2}{1 - \mathbf{s}^2} \right\rangle - \left\langle \frac{\mathbf{a}\mathbf{r}}{1 - \mathbf{s}^2} \right\rangle^2 \geq 0,$$

so that $D(\cdot, \mathbf{s})$ is always positive.

Figure 6 shows that the approximations, together with the continuum limit expressions found in the main text, are valid to high accuracy over broad ranges of N .

D Impact of pure correlation stimulus dependence on I_F^{cov} .

We show that the impact of stimulus dependence of correlations on I_F^{cov} is relatively small compared to the impact on I_F^{mean} in the situation discussed in Section 4. By invoking the symmetry of the tuning curves again

$$D(Gs, s) = D\left(s'(\theta) + \frac{v'(\theta)}{v(\theta)}s(\theta), s(\theta)\right) \sim \frac{N}{2\pi} \int_0^{2\pi} \left(s'(\phi) + \frac{v'(\phi)}{v(\phi)}s(\phi) \right)^2 \frac{1}{1 - s^2(\phi)} d\phi, \quad (27)$$

where $s'(\theta)$ is typically much smaller than $s(\theta)v'(\theta)/v(\theta)$. The term $D(Gs, s)$ appearing in I_F^{cov} is therefore of second order in $s(\theta)$ and hence negligible compared to I_F^{mean} . For typical parameters,

the difference is greater than an order of magnitude.

The last term in the Fisher information comes from the sum in I_F^{cov} given by Eq. (26). In the continuum limit this term is approximately

$$\frac{N}{2\pi} \int_0^{2\pi} \left(\frac{v(\phi)}{2v'(\phi)} - \frac{s'(\phi)s(\phi)}{1-s^2(\phi)} \right)^2 d\phi = \frac{N}{4\pi} \int_0^{2\pi} \left(\frac{d}{d\phi} [\log(v(\phi)(1-s^2(\phi)))] \right)^2 d\phi.$$

For the type of stimulus dependence that we assume $\frac{v(\phi)}{2v'(\phi)}$ and $-\frac{s'(\phi)s(\phi)}{1-s^2(\phi)}$ have opposite signs. For small correlations, the first term will dominate and stimulus dependence of correlations will decrease this entry in I_F^{cov} . When correlations are not perfect (near 1) the term I_F^{var} is typically much smaller than I_F^{mean} .

E Details of the numerical implementations

Numerical values of Fisher Information in Figs. 3 and 5 were found by directly inverting the correlation matrices Q and performing the required matrix multiplications in MATLAB. The authors are happy to provide these codes upon request.

The procedure is as follows: We first fix the average value of correlations, $\langle \rho_{ij} \rangle$, among all neurons in the population (the value $\langle \rho_{ij} \rangle = 0.1$ was used for all figures in this paper). Next, we define correlation matrices consistent with this value of $\langle \rho_{ij} \rangle$, for two cases, *Stimulus Dependent (SD)* and *Stimulus Independent (SI)* (see main text). We first define $Q_{i,j}$ via Eqn. (2), assuming that the $\rho_{i,j}(\theta)$ are given by (3). Here, for Figs. 3 and 5, we used $s(\theta) = k_\rho + b_\rho a^2(\theta)$, where $a(\theta) = 1/2(1 + \cos(\theta))$ and k_ρ and b_ρ are constants chosen as follows: (i) the average correlation $\langle \rho_{ij} \rangle = 0.1$, and (ii) the ratio of largest so smallest pairwise correlations, $(k_\rho + b_\rho)^2/b_\rho^2$, should be $R = 10$ for the SD case and $R = 0$ (i.e., $b_\rho = 0$) for the SI case.

To study the affects of heterogeneity, as a final step we jitter the tuning curves for s and v by $\pm 20\%$.

References

- [1] L. F. Abbott and P. Dayan. The effect of correlated variability on the accuracy of a population code. *Neural Comput*, 11(1):91–101, 1999.
- [2] E. Aksay, R. Baker, H.S. Seung, and D.W. Tank. Correlated discharge among cell pairs within the oculomotor horizontal velocity-to-position integrator. *J Neurosci*, 23(34):10852–10858, 2003.
- [3] B. B. Averbeck, P. E. Latham, and A. Pouget. Neural correlations, population coding and computation. *Nat Rev Neurosci*, 7(5):358–366, 2006.
- [4] B. B. Averbeck and D. Lee. Neural Noise and Movement-Related Codes in the Macaque Supplementary Motor Area. *J Neurosci*, 23(20):7630–7641, 2003.
- [5] B. B. Averbeck and D. Lee. Coding and transmission of information by neural ensembles. *Trends Neurosci*, 27(4):225–230, 2004.

- [6] B. B. Averbeck and D. Lee. Effects of noise correlations on information encoding and decoding. *J Neurophys*, 95:3633–3644, 2006.
- [7] J. Biederlack, M. Castelo-Branco, S. Neuenschwander, D. W. Wheeler, W. Singer, and D. Nikolić. Brightness induction: rate enhancement and neuronal synchronization as complementary codes. *Neuron*, 52(6):1073–1083, 2006.
- [8] M. D. Binder and R. K. Powers. Relationship Between Simulated Common Synaptic Input and Discharge Synchrony in Cat Spinal Motoneurons. *J Neurophysiol*, 86(5):2266–2275, 2001.
- [9] K. H. Britten, M. N. Shadlen, W. T. Newsome, and J. A. Movshon. The analysis of visual motion: a comparison of neuronal and psychophysical performance. *J Neurosci*, 12(12):4745–4765, 1992.
- [10] D. A. Butts and M. S. Goldman. Tuning curves, neuronal variability, and sensory coding. *PLoS Biol*, 4(4):e92, 2006.
- [11] M. J. Chacron and J. Bastian. Population Coding by Electrosensory Neurons. *J Neurophys*, 99(4):1825–1835, 2008.
- [12] M. I. Chelaru and V. Dragoi. Neuronal response heterogeneity improves the efficiency of population coding. To appear in *P Natl Acad Sci USA*, 2008.
- [13] Y. Chen, W. S. Geisler, and E. Seidemann. Optimal decoding of correlated neural population responses in the primate visual cortex. *Nat Neurosci*, 9(11):1412–1420, 2006.
- [14] T. M. Cover and J. A. Thomas. *Elements of information theory*. Wiley in Telecommunications. John Wiley & Sons Inc., New York, 1991. A Wiley-Interscience Publication.
- [15] H. Cramer. *Mathematical Methods of Statistics*. Princeton Univ. Press, 1946.
- [16] P. Dayan and L. F. Abbott. *Theoretical neuroscience: computational and mathematical modeling of neural systems*. MIT Press, Cambridge, MA, 2001.
- [17] J. de la Rocha, B. Doiron, E. Shea-Brown, K. Josić, and A. Reyes. Correlation between neural spike trains increases with firing rate. *Nature*, 448(7155):802–806, 2007.
- [18] R. C. deCharms and M. M. Merzenich. Primary cortical representation of sounds by the coordination of action potentials. *Nature*, 381:610–613, 1996.
- [19] J. W. Demmel. *Applied Numerical Linear Algebra*. Society for Industrial & Applied Mathematics, Philadelphia, PA, 1997.
- [20] N. Ghisovan, A. Nemri, S. Shumikhina, and S. Molotchnikoff. Synchrony between orientation-selective neurons is modulated during adaptation-induced plasticity in cat visual cortex. *BMC Neuroscience*, 9(1):60, 2008.
- [21] C. M. Gray, P. Köing A. K. Engel, and W. Singer. Oscillatory responses in cat visual cortex exhibit inter-columnar synchronization which reflects global stimulus properties. *Nature*, 338:334–337, 1989.

- [22] D. S. Greenberg, A. R. Houweling, and J. N. D. Kerr. Population imaging of ongoing neuronal activity in the visual cortex of awake rats. *Nat Neurosci*, 11(7):749–751, 2008.
- [23] D. A. Gutnisky and V. Dragoi. Adaptive coding of visual information in neural populations. *Nature*, 452(7184):220–4, 2008.
- [24] K. O. Johnson. Sensory discrimination: neural processes preceding discrimination decision. *J Neurophys*, 43(6):1793–1815, 1980.
- [25] S. M. Kay. *Fundamentals of statistical signal processing: estimation theory*. Prentice-Hall, Inc., Upper Saddle River, NJ, USA, 1993.
- [26] A. Kohn and M. A. Smith. Stimulus dependence of neuronal correlation in primary visual cortex of the macaque. *J Neurosci*, 25(14):3661–3673, 2005.
- [27] A. Kohn, M. A. Smith, and J. A. Movshon. Effect of prolonged and rapid adaptation on correlation in V1. *Computational and Systems Neuroscience, Cold Spring Harbor NY (abstract)*, 2004.
- [28] D. Lee, N. L. Port, W. Kruse, and A. P. Georgopoulos. Variability and correlated noise in the discharge of neurons in motor and parietal areas of the primate cortex. *J Neurosci*, 18(3):1161–1170, 1998.
- [29] C. D. Meyer. *Matrix Analysis and Applied Linear Algebra*. Society for Industrial & Applied Mathematics, Philadelphia, PA, 2000.
- [30] F. Montani, A. Kohn, M. A. Smith, and S. R. Schultz. How do stimulus-dependent correlations between v1 neurons affect neural coding? *Neurocomputing*, 70:1782–1787, 2007.
- [31] M. W. Oram, P. Földiák, D. I. Perrett, and F. Sengpiel. The ‘Ideal Homunculus’: decoding neural population signals. *Trends Neurosci*, 21(6):259–265, 1998.
- [32] S. Panzeri, S. Schultz, A. Treves, and E. T. Rolls. Correlations and the encoding of information in the nervous system. *Proc Royal Soc Lond B*, 266:1001–1012, 1999.
- [33] R. S. Petersen, S. Panzeri, and M. E. Diamond. Population Coding of Stimulus Location in Rat Somatosensory Cortex. *Neuron*, 32(3):503–514, 2001.
- [34] J. Poort and P. R. Roelfsema. Noise correlations have little influence on the coding of selective attention in area v1. *Cerebral Cortex*, 2008. Advanced Online Publication.
- [35] C. Rao. Information and the accuracy attainable in the estimation of statistical parameters. *Bull. Calcutta Math. Soc.*, 37:81–89, 1945.
- [36] E. T. Rolls, L. Franco, N. C. Aggelopoulos, and S. Reece. An Information Theoretic Approach to the Contributions of the Firing Rates and the Correlations Between the Firing of Neurons. *J Neurophys*, 89(5):2810–2822, 2003.
- [37] R. Romo, A. Hernandez, A. Zainos, and E. Salinas. Correlated neuronal discharges that increase coding efficiency during perceptual discrimination. *Neuron*, 38(4):649–657, 2003.

- [38] J. M. Samonds, J. D. Allison, H. A. Brown, and A. B. Bonds. Cooperation between Area 17 Neuron Pairs Enhances Fine Discrimination of Orientation. *J Neurosci*, 23(6):2416, 2003.
- [39] J. M. Samonds, J. D. Allison, H. A. Brown, and A. B. Bonds. Cooperative synchronized assemblies enhance orientation discrimination. *P Natl Acad Sci USA*, 101(17):6722, 2004.
- [40] P. Seriès, P. E. Latham, and A. Pouget. Tuning curve sharpening for orientation selectivity: coding efficiency and the impact of correlations. *Nat Neurosci*, 7:1129 – 1135, 2004.
- [41] H. S. Seung and H. Sompolinsky. Simple models for reading neuronal population codes. *P Natl Acad Sci USA*, 90(22):10749–10753, 1993.
- [42] M. Shamir and H. Sompolinsky. Correlation codes in neuronal populations. *Advances in Neural Information Processing Systems*, 14:277–284, 2001.
- [43] M. Shamir and H. Sompolinsky. Nonlinear population codes. *Neural Comput*, 16(6):1105–1136, 2004.
- [44] M. Shamir and H. Sompolinsky. Implications of neuronal diversity on population coding. *Neural Comput*, 18(8):1951–1986, 2006.
- [45] E. Shea-Brown, K. Josić, B. Doiron, and J. de la Rocha. Correlation and synchrony transfer in integrate-and-fire neurons: Basic properties and consequences for coding. *Phys Rev Lett*, 100:108102, 2008.
- [46] H. Sompolinsky, H. Yoon, K. Kang, and M. Shamir. Population coding in neuronal systems with correlated noise. *Phys Rev E*, 64(5 Pt 1):051904, 2001.
- [47] E. Vaadia, I. Haalman, M. Abeles, H. Bergman, Y. Prut, H. Slovin, and A. Aertsen. Dynamics of neuronal interactions in monkey cortex in relation to behavioural events. *Nature*, 373(6514):515–518, 1995.
- [48] S. D. Wilke and C. W. Eurich. Representational accuracy of stochastic neural populations. *Neural Comput*, 14(1):155–189, 2002.
- [49] E. Zohary, M. Shadlen, and W. Newsome. Correlated neuronal discharge rate and its implications for psychophysical performance. *Nature*, 370:140–143, 1994.